Advanced Science Letters
Vol. 2, 455–458, 2009

An Optical Scheme for the Generation and Analysis of a Two Photon Six-Qubit Linear Cluster State

Raino Ceccarelli[1], Giuseppe Vallone[1,2], Francesco De Martini[1,2,3], and Paolo Mataloni[1,2,*]

[1]*Dipartimento di Fisica della Sapienza Università di Roma, Roma, 00185 Italy*
[2]*Consorzio Nazionale Interuniversitario per le Scienze, Fisiche della Materia, Roma, 00185 Italy*
[3]*Accademia Nazionale dei Lincei, via della Lungara 10, Roma 00165, Italy*

We present the project of an optical scheme that allows to engineer a 2-photon 6-qubit linear cluster state. By this scheme we are able to create a hyperentangled state based on polarization, linear momentum and arrival time entanglement. Since the three degrees of freedom of the photons are fully independent, the hyperentangled state allows the maximum entanglement of the particles. By suitable local unitary operations the hyperentangled state can be easily transformed into a linear cluster state, with important applications in photonic quantum computation and quantum nonlocality tests.

1. REALIZATION OF THE $|LC_6\rangle$ STATE

Measurement-based quantum computation requires the generation of a particular class of n-qubit entangled states, the cluster states.[1,2] The number n of qubits requested in a cluster state becomes larger and larger with the increase of complexity of quantum algorithms. The implementation of cluster states with n qubits encoded in some degrees of freedom of n photons can be extremely difficult due to the low efficiency of multi-photon interactions. Indeed, the experimental preparations of 6-qubit 6-photon cluster states realized so far[3] presented low entanglement visibilities. We present here the proposal of an experimental setup allowing to generate and analyze a 6-qubit linear cluster state based on two photons, namely Alice (A) and Bob (B), hyperentangled in longitudinal momentum, arrival-time and polarization. The six-qubit linear cluster state ($|LC_6\rangle$) is the state associated to the graph shown in Figure 1. It is defined as the unique common eigenstate with eigenvalue $+1$ of the set of independent observables $g_i = X_i \prod_{j\in N_i} Z_j$, where X_i and Z_i denote the Pauli matrices σ_x and σ_z acting on qubit i, and N_i is the set of neighbors connected to i. It is well known that the explicit expression of the state $|LC_6\rangle$ is obtained by applying to the initial state $|+\rangle^{\otimes 6}$ a CZ_{ij} (i.e., a Control-Z gate) between each couple $\{i, j\}$ of connected vertices. Following this procedure the state associated to the graph shown in Figure 1(I) can be explicitly written as:

$$\begin{aligned}|LC_6\rangle &= \frac{1}{2\sqrt{2}}(|0\rangle_1|0\rangle_2|+\rangle_3|+\rangle_4|+\rangle_5|0\rangle_6 + |0\rangle_1|0\rangle_2|-\rangle_3|+\rangle_4|-\rangle_5|1\rangle_6 \\ &+ |0\rangle_1|1\rangle_2|+\rangle_3|+\rangle_4|-\rangle_5|0\rangle_6 + |0\rangle_1|1\rangle_2|-\rangle_3|+\rangle_4|+\rangle_5|1\rangle_6 \\ &+ |1\rangle_1|0\rangle_2|+\rangle_3|-\rangle_4|+\rangle_5|0\rangle_6 + |1\rangle_1|0\rangle_2|-\rangle_3|-\rangle_4|-\rangle_5|1\rangle_6 \\ &- |1\rangle_1|1\rangle_2|+\rangle_3|-\rangle_4|-\rangle_5|0\rangle_6 - |1\rangle_1|1\rangle_2|-\rangle_3|-\rangle_4|+\rangle_5|1\rangle_6)\end{aligned} \quad (1)$$

The experimental scheme that we are going to investigate is based on the physical implementation of a quantum state ($|C_6\rangle$) LC equivalent[a] to $|LC_6\rangle$. $|C_6\rangle$ is defined as:

$$\begin{aligned}|C_6\rangle &= \frac{CZ_{12}CX_{65}}{2\sqrt{2}}(|0\rangle_1|0\rangle_4 + |1\rangle_1|1\rangle_4) \otimes (|0\rangle_2|0\rangle_5 + |1\rangle_2|1\rangle_5) \\ &\otimes (|0\rangle_3|1\rangle_6 + |1\rangle_3|0\rangle_6)\end{aligned} \quad (2)$$

and it is related to the $|LC_6\rangle$ state by:

$$|LC_6\rangle = \mathcal{U}_L|C_6\rangle \quad (3)$$

In the previous equations, CX_{65} represents the Controlled-X gate between qubits 6 (control) and 5 (target), while $\mathcal{U}_L = H_5H_3X_3H_4$ with H_j the Hadamard gate $H = (1/\sqrt{2})(X + Z)$ acting on qubit j. The LC equivalence between $|C_6\rangle$ and $|LC_6\rangle$ allows a one-to-one correspondence between the measurement observables on $|C_6\rangle$ and on $|LC_6\rangle$ states (see Table I).

The proposed experimental setup is an evolution of the two-photon hyper-entangled (in momentum and polarization) state

[a]Two n-qubit states $|\psi\rangle$ and $|\psi'\rangle$ are defined local unitary (LU) equivalent if there exists an LU operation $\mathcal{U}_n = \bigotimes_{i=1}^n U_i$ which maps $|\psi'\rangle$ to $|\psi\rangle$. Two n-qubit states $|\psi\rangle$ and $|\psi'\rangle$ are said to be local Clifford (LC) equivalent if they are LU equivalent, and the $\mathcal{U}_n$ operation, which transforms $|\psi'\rangle$ into $|\psi\rangle$, maps the Pauli group into itself.

*Author to whom correspondence should be addressed.

 1936-6612/2009/2/455/004 doi:10.1166/asl.2009.1049

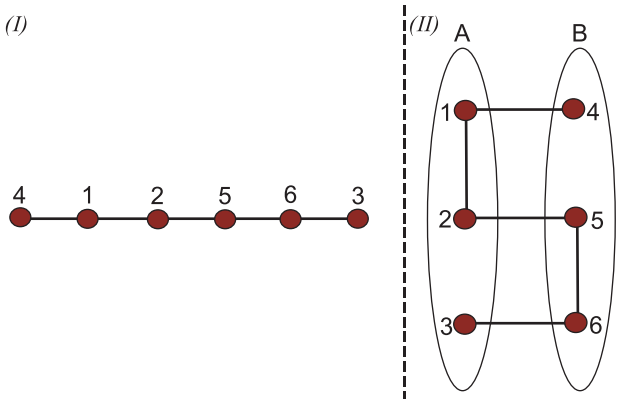

Fig. 1. (I) Graph associated to the six-qubit linear cluster state. (II) In the two-photon realization three qubits (1, 2 and 3) are encoded in the photon *A* and three (4, 5 and 6) in the photon *B*. For each photon each vertex corresponds to a different degree of freedom.

source shown in Figure 2. The state generated by this source is expressed in the following way (see Refs. [4–6] for more details):

$$\frac{1}{\sqrt{2}}(|H\rangle_A|H\rangle_B+|V\rangle_A|V\rangle_B)\otimes\frac{1}{\sqrt{2}}(|r\rangle_A|\ell\rangle_B+|\ell\rangle_A|r\rangle_B) \quad (4)$$

where $|H\rangle_j$ ($|V\rangle_j$) and $|\ell\rangle_j$ ($|r\rangle_j$) respectively represents the horizontal (vertical) polarization and the left (right) path of the photon j. In order to produce $|C_6\rangle$ it is necessary to encode two more qubits in an additional degree of freedom of the two photons. This can be implemented by using the interferometric scheme (see Fig. 2(right)) recently proposed to create arrival time (i.e., time-energy) entanglement of two photon states.[7] Basically, it is a revised version of the Franson's[8] interferometric scheme where instead of two unbalanced interferometers, we adopt a single Michelson interferometer (MI) operating simultaneously for the two photons. They are emitted at degenerate wavelength by spontaneous parametric down conversion SPDC (pumped by a continuous wave laser) in a Type I phase matched nonlinear (NL) crystal and injected into the MI.

In this setup the same beam splitter (BS) is used both for the preparation of the state in the first passage of the photons and for the final measurement in the second passage. Photons, whose directions are carefully selected by two masks, can travel along the Short (S) or Long (L) path, after the first partition occurring on the BS. After reflection by mirrors, each photon experiences a new BS reflection-transmission process with relative path delay $\Delta x_0 = 2(L-S)$. The BS output beams are then detected by single photon detectors. The relative phase of the path contributions

Table I. LC equivalence between $|C_6\rangle$ and $|LC_6\rangle$ Pauli operators.

Photon A		Photon B	
$\|LC_6\rangle$	$\|C_6\rangle$	$\|LC_6\rangle$	$\|C_6\rangle$
X_1	X_1	X_4	Z_4
Y_1	Y_1	Y_4	$-Y_4$
Z_1	Z_1	Z_4	X_4
X_2	Z_2	X_5	X_5
Y_2	$-Y_2$	Y_5	Y_5
Z_2	X_2	Z_5	Z_5
X_3	Z_3	X_6	X_6
Y_3	$-Y_3$	Y_6	$-Y_6$
Z_3	X_3	Z_6	$-Z_6$

$|S_A, S_B\rangle$ and $|L_A, L_B\rangle$ can be tuned by a piezo transducer that finely changes the mirror position in the long arm. Interesting enough, this single MI configuration allows to minimize the state phase instabilities.

The key element of this setup is represented by the swapping operation between the two photon paths, performed in the L arm of MI. It is realized by a lens (see Fig. 2(right)) aligned at a distance exactly equal to its focal length from mirror. By this configuration we are able to detect coincidences only if both photons travel along the same arm of MI after the first interaction with BS. In fact if, for instance, the first photon passes through the L path and the second follows the S path (i.e., if we consider the event $|L\rangle_A|S\rangle_B$), after the second interaction with BS they will end on the same detector. Thus no coincidence is detected in this case. The same happens with the $|S\rangle_A|L\rangle_B$ event.

By this setup it is no longer necessary to perform the nonlocal temporal post-selection which is needed in the Franson's scheme to discard the events $|L\rangle_A|S\rangle_B$ and $|S\rangle_A|L\rangle_B$. By our scheme they are simply rejected by the coincidence measurement. A scheme similar to the one presented in this article has been recently proposed for a conclusive energy-time Bell test of local realism.[9]

Going back to the scheme conceived for the generation of the 6-qubit hyperentangled state, the basic idea is to inject the state created by the source of Figure 2(left) into the Michelson interferometer. After the first passage of photons through the BS the following state is generated:

$$\frac{1}{\sqrt{2}}(|L\rangle_A|L\rangle_B+|S\rangle_A|S\rangle_B)\otimes\frac{1}{\sqrt{2}}(|H\rangle_A|H\rangle_B+|V\rangle_A|V\rangle_B)$$
$$\otimes\frac{1}{\sqrt{2}}(|r\rangle_A|\ell\rangle_B+|\ell\rangle_A|r\rangle_B) \quad (5)$$

Under the correspondence $|L\rangle_{A,B}\leftrightarrow|0\rangle_{1,4}$, $|S\rangle_{A,B}\leftrightarrow|1\rangle_{1,4}$, $|H\rangle_{A,B}\leftrightarrow|0\rangle_{2,5}$, $|V\rangle_{A,B}\leftrightarrow|1\rangle_{2,5}$, $|\ell\rangle_{A,B}\leftrightarrow|0\rangle_{3,6}$, $|r\rangle_{A,B}\leftrightarrow|1\rangle_{3,6}$, we note that by performing a CX_{65} and a CZ_{12} to our state, the generated state is equivalent to $|C_6\rangle$ expressed in the logical basis $|0\rangle$ and $|1\rangle$.[b] It is worth stressing that the two Controlled operations act only on single photon degrees of freedom. In this sense they are local and can be easily implemented by linear optics. At the same time these operations act on the two qubits associated to a single photon.

The CX_{65} is obtained by inserting a $\lambda/2$ waveplate (HW) at $\pi/2$ intercepting the mode r_A, while the CZ_{12} is performed by the insertion on the modes S_A and S_B of a $\lambda/4$ (QWP) at $\pi/4$ followed by a QWP at $\pi/4$ only on the S_A, and a QWP at 0 on mode S_B. In this way we have implemented the $|C_6\rangle$ state.

2. ANALYSIS OF THE $|LC_6\rangle$ STATE

The measurement apparatus proposed to analyze the $|C_6\rangle$ state is sketched in Figure 3. In the scheme we have included the MI interferometer that creates the time-energy entanglement. As a matter of fact its generation takes place just before the second passage of the photons through the BS, while the interferometer output state corresponds to the projection of $|C_6\rangle$ on the $|L\rangle_{A,B}\pm|S\rangle_{A,B}$ basis. Two thin glass plates suitably inserted on the MI short arm allow the projection on the $|L\rangle_{A,B}\pm i|S\rangle_{A,B}$ basis. The

[b] As shown in the appendix, the cluster state can be equivalently generated by applying a CZ_{56} and a CX_{12} transformation.

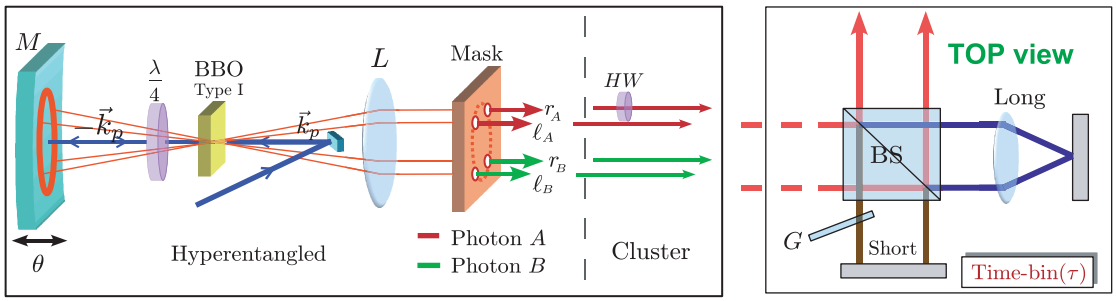

Fig. 2. (left) Scheme of the polarization-momentum hyperentanglement source: the polarization entangled state $|\Phi\rangle = 1/\sqrt{2}(|H\rangle_A|H\rangle_B + e^{i\theta}|V_1, V_2\rangle)$ arises from the superposition of the degenerate emission cones of a type-I BBO crystal shined in two opposite directions by a continuous wave Argon laser. The basic elements of the source are: a spherical mirror M, reflecting both the parametric radiation and the pump beam. Its micrometric displacement allows to control the state phase θ ($\theta = 0, \pi$); a $\lambda/4$ waveplate, placed within the M-BBO path, performing the $|H\rangle_A|H\rangle_B \rightarrow |V\rangle_A|V\rangle_B$ transformation on the two-photon state belonging to the left cone; a positive lens which transforms the conical parametric emission of the crystal into a cylindrical one. Four longitudinal k-modes are selected by a four hole mask. The $\lambda/2$ waveplate HW intercepting the mode r_A performs the CX_{65} operations. (right) Energy-time entanglement allowed by the long pump coherence time is obtained with a modified Michelson interferometer interchanging the *A* and *B* modes in the Long path. Thin glass plates (*G*) are used to set the basis of the energy-time measurement.

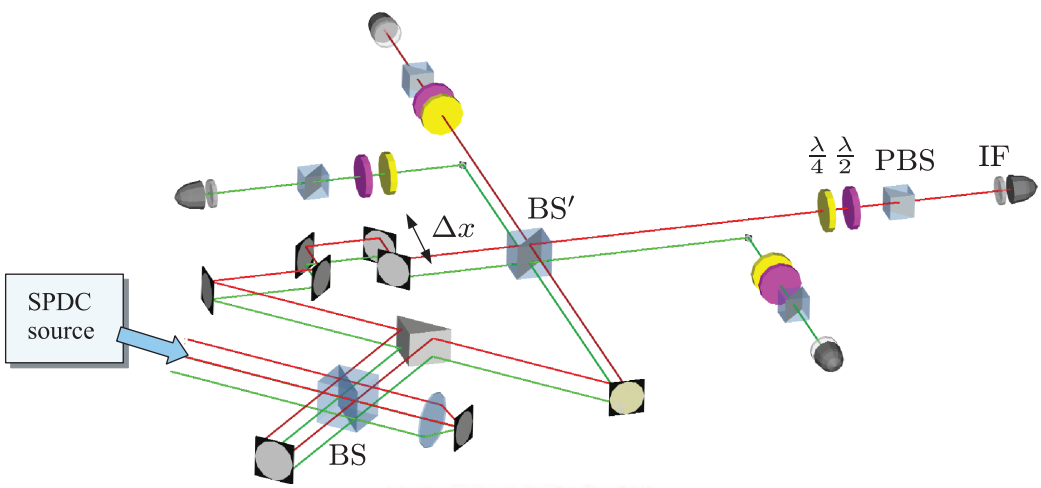

Fig. 3. Measurement scheme: the SPDC radiation corresponding to the polarization-momentum hyperentangled state is injected into a Michelson interferometer allowing the further time-energy entanglement. The BS in the first passage of the photon generates the energy-time entanglement while in the second passage acts as a measurement device. The momentum measurement apparatus is composed by two arms that match on the BS′. A micrometric stage allows the path variation Δx. The photon wavelength is selected by interferometric filters (IF) placed in front of the detectors. Polarization analysis is performed by standard tomographic systems ($\lambda/4$, $\lambda/4$, and PBS).

measurement in the standard computational basis can be easily implemented by blocking the photons that pass through one of the two MI arms.

The momentum measurements are performed in a very similar way. The two mode pairs $\ell_A - r_B$ and $r_A - \ell_B$ emerging from the MI, are spatially and temporally combined onto a 50% beam splitter (BS′) by an interferometric apparatus, where a trombone mirror assembly allows fine delay adjustment Δx. By suitable tilting of two thin glass plates inserted on one arm of the interferometer, we can separately set the relative phase of the A and B modes matching on BS′.

Polarization analyses are performed by standard tomographic apparatus on each detector arm, given by a sequence of $\lambda/4 - \lambda/2$ waveplates and a polarizing beam splitter (PBS).

3. CONCLUSIONS

In this article we proposed an optical scheme for the generation of a 6-qubit 2-photon cluster state. The method is based on the local manipulation of a polarization-momentum-energy/time hyperentangled state generated by a SPDC source. The cluster states can be generated at high repetition rate thanks to the high production rate (∼10 KHz) of the photon pair. The $|LC_6\rangle$ cluster state allows to span a high dimension Hilbert space. Because of this reason it has relevant applications both for the one-way model of quantum computation and for advanced tests of quantum mechanics since it has been demonstrated that the quantum nonlocality of a state grows with its size.

4. APPENDIX: CALCULATIONS

In this section we report some useful calculations of equivalent expressions of the $|LC_6\rangle$ state. Remembering that:

$$CZ_{ij}|+\rangle_i|+\rangle_j = \frac{1}{\sqrt{2}}(|0\rangle_i|+\rangle_j + |1\rangle_i|-\rangle_j)$$
$$= \frac{1}{\sqrt{2}}(|+\rangle_i|0\rangle_j + |-\rangle_i|1\rangle_j) = CZ_{ji}|+\rangle_i|+\rangle_j \quad (6)$$

we have:

$$|LC_6\rangle = CZ_{14}CZ_{12}CZ_{25}CZ_{56}CZ_{36}|+\rangle_1|+\rangle_2|+\rangle_3|+\rangle_4|+\rangle_5|+\rangle_6$$
$$= CZ_{12}CZ_{56}\frac{1}{2\sqrt{2}}(|0\rangle_1|+\rangle_4+|1\rangle_1|-\rangle_4)$$
$$\otimes(|0\rangle_2|+\rangle_5+|1\rangle_2|-\rangle_5)\otimes(|0\rangle_3|+\rangle_6+|1\rangle_3|-\rangle_6) \quad (7)$$

If we define $|\phi^+\rangle_{ij} \equiv 1/\sqrt{2}(|0\rangle_i|0\rangle_j+|1\rangle_i|1\rangle_j)$, from the last expression it is easy to check the equivalence of the following ones:

$$\begin{aligned}|LC_6\rangle &= CZ_{12}CZ_{56}H_1H_2H_3|\phi^+\rangle_{14}\otimes|\phi^+\rangle_{25}\otimes|\phi^+\rangle_{36}\\ &= CZ_{12}CZ_{56}H_1H_5H_3|\phi^+\rangle_{14}\otimes|\phi^+\rangle_{25}\otimes|\phi^+\rangle_{36}\\ &= CZ_{12}CZ_{56}H_1H_5H_6|\phi^+\rangle_{14}\otimes|\phi^+\rangle_{25}\otimes|\phi^+\rangle_{36}\\ &= CZ_{12}CZ_{56}H_1H_2H_6|\phi^+\rangle_{14}\otimes|\phi^+\rangle_{25}\otimes|\phi^+\rangle_{36}\\ &= CZ_{12}CZ_{56}H_4H_2H_3|\phi^+\rangle_{14}\otimes|\phi^+\rangle_{25}\otimes|\phi^+\rangle_{36}\\ &= CZ_{12}CZ_{56}H_4H_5H_3|\phi^+\rangle_{14}\otimes|\phi^+\rangle_{25}\otimes|\phi^+\rangle_{36}\\ &= CZ_{12}CZ_{56}H_4H_5H_6|\phi^+\rangle_{14}\otimes|\phi^+\rangle_{25}\otimes|\phi^+\rangle_{36}\\ &= CZ_{12}CZ_{56}H_4H_2H_6|\phi^+\rangle_{14}\otimes|\phi^+\rangle_{25}\otimes|\phi^+\rangle_{36} \quad (8)\end{aligned}$$

By using the relations

$$ZH = HX, \qquad CZ_{ij} = \frac{\mathbb{1}_i+Z_i}{2}\otimes\mathbb{1}_j + \frac{\mathbb{1}_i-Z_i}{2}\otimes Z_j \quad (9)$$

we can show that

$$CZ_{ij}H_j = H_jCX_{ij} = \widetilde{CZ}_{ji}, \qquad CZ_{ij}H_i = H_iCX_{ji} = \widetilde{CZ}_{ij} \quad (10)$$

where $\widetilde{CZ}_{ji}$ stands for the controlled-Z transformation acting on qubit i when the control qubit j is in the state $|0\rangle$ instead of $|1\rangle$).

The previous equations can be used to show that

$$\begin{aligned}|LC_6\rangle &= (H_4H_3H_5X_3)CZ_{12}CX_{65}\frac{1}{2\sqrt{2}}(|0\rangle_1|0\rangle_4+|1\rangle_1|1\rangle_4)\\ &\quad\otimes(|0\rangle_2|0\rangle_5+|1\rangle_2|1\rangle_5)\otimes(|0\rangle_3|1\rangle_6+|1\rangle_3|0\rangle_6)\\ |LC_6\rangle &= (H_4H_3H_2X_3)CX_{12}CZ_{56}\frac{1}{2\sqrt{2}}(|0\rangle_1|0\rangle_4+|1\rangle_1|1\rangle_4)\\ &\quad\otimes(|0\rangle_2|0\rangle_5+|1\rangle_2|1\rangle_5)\otimes(|0\rangle_3|1\rangle_6+|1\rangle_3|0\rangle_6)\end{aligned} \quad (11)$$

Acknowledgments: This paper is published despite the effects of the Italian law 133/08 (http://groups.google.it/group/scienceaction). This law drastically reduces public funds to public Italian universities, which is particularly dangerous for scientific free research, and it will prevent young researchers from getting a position, either temporary or tenured, in Italy. The authors are protesting against this law to obtain its cancellation.

References and Notes

1. H. J. Briegel and R. Raussendorf, *Phys. Rev. Lett.* 86, 910 **(2001)**.
2. R. Raussendorf and H. J. Briegel, *Phys. Rev. Lett.* 86, 5188 **(2001)**.
3. C.-Y. Lu, X.-Q. Zhou, O. Gühne, W.-B. Gao, J. Zhang, Z.-S. Yuan, A. Goebel, T. Yang, and J.-W. Pan, *Nature Phys.* 3, 91 **(2007)**.
4. M. Barbieri, F. De Martini, P. Mataloni, G. Vallone, and A. Cabello, *Phys. Rev. Lett.* 97, 140407 **(2006)**.
5. C. Cinelli, M. Barbieri, R. Perris, P. Mataloni, and F. De Martini, *Phys. Rev. Lett.* 95, 240405 **(2005)**.
6. M. Barbieri, C. Cinelli, P. Mataloni, and F. De Martini, *Phys. Rev. A* 72, 052110 **(2005)**.
7. A. Rossi, G. Vallone, F. De Martini, and P. Mataloni, *Phys. Rev. A* 78, 012345 **(2008)**.
8. J. D. Franson, *Phys. Rev. Lett.* 62, 2205 **(1989)**.
9. A. Cabello, A. Rossi, G. Vallone, F. De Martini, and P. Mataloni, *Phys. Rev. Lett.* 102, 040401 **(2009)**.

Received: 22 October 2008. Accepted: 11 November 2008.